

1 **Light-mediated circuit switching in the *Drosophila* neuronal clock network**

2 Schlichting M^{1*}, Weidner P^{1,2}, Diaz M¹, Menegazzi P², Dalla-Benetta E², Helfrich-Förster

3 C^{2*}, Rosbash M¹.

4

5 1 Howard Hughes Medical Institute and Department of Biology, Brandeis University,

6 Waltham, MA 02454 USA

7 2 University of Würzburg, Department for Neurobiology and Genetics, Am Hubland, 97074

8 Würzburg

9

10 * Correspondence should be addressed to charlotte.foerster@uni-wuerzburg.de or

11 mschlichting@brandeis.edu

12 **Summary (150 word limit)**

13 The circadian clock is a timekeeper but also helps adapt physiology to the outside world. This
14 is because an essential feature of clocks is their ability to adjust (entrain) to the environment,
15 with light being the most important signal. Whereas Cryptochrome-mediated entrainment is
16 well understood in *Drosophila*, integration of light information via the visual system lacks a
17 neuronal or molecular mechanism. Here we show that a single photoreceptor sub-type is
18 essential for long day adaptation. These cells activate key circadian neurons, namely the
19 ILNvs, which release the neuropeptide PDF. Using a cell-specific CRISPR/Cas9 assay, we
20 show that PDF directly interacts with neurons important for evening (E) activity timing.
21 Interestingly, this pathway is specific for light entrainment and appears to be dispensable in
22 constant darkness (DD). The results therefore indicate that external cues cause a
23 rearrangement of neuronal hierarchy, which is a novel form of plasticity.

24 **Introduction**

25 Circadian clocks evolved as an adaptation to the continuous change of day and night and are
26 believed to provide organisms a fitness advantage. The underlying molecular machinery
27 includes a transcriptional-translational feedback loop, which generates oscillations of clock
28 gene expression with an endogenous period close to 24 hours (circa=about; dies=day)
29 (Hardin, 2011). This period is approximately 24.2h in humans, whereas a *Drosophila* period
30 was reported to be 23.8h (Czeisler et al., 1999; Dubowy and Sehgal, 2017). A key feature of
31 circadian clocks is the ability to entrain to the 24h environment. This means that the human
32 clock has to be accelerated by about 0.2h each day, whereas this *Drosophila* clock has to be
33 slowed down to the same extent. To do so, clocks must integrate external cues, so called
34 zeitgebers, which are used to synchronize the molecular and physiological properties of the
35 organism (Golombek and Rosenstein, 2010).

36 The most important zeitgeber is light. In mammals, a combination of the traditional
37 photoreception pathway (rods and cones) and the circadian photoreceptor melanopsin in
38 retinal ganglion cells allows for fine-tuning of clock synchronization (Berson et al., 2002;
39 Hattar et al., 2002; Lucas et al., 2012). Similarly, *Drosophila* uses the visual system and the
40 circadian photoreceptor Cryptochrome (CRY) for light synchronization (Rieger et al., 2003;
41 Stanewsky et al., 1998). CRY-mediated entrainment is well understood in *Drosophila*,
42 whereas less is known about the mechanism of entrainment via the visual system. It consists
43 of seven eye structures: three ocelli, two Hofbauer-Buchner-eyelets and two compound eyes
44 (Hofbauer and Buchner, 1989).

45 The compound eye consists of approximately 800 ommatidia, each harboring 8
46 photoreceptor cells (Rs): R1-6 are located in the periphery and span the whole depth of the
47 ommatidium. These cells were previously shown to be important for motion vision and
48 express Rhodopsin 1 (Rh1) (Yamaguchi et al., 2008). In the center, R7 is located above R8.

49 These cells have a complex expression pattern of Rh4 and/or Rh3 in R7 and Rh5 or Rh6 in
50 R8 (Rister et al., 2013). How light information is conveyed from these photoreceptor cells to
51 the circadian clock is not well understood.

52 The *Drosophila* clock neuron network consists of 150 clock neurons distributed in the
53 lateral and dorsal parts of the brain. Recent electrophysiological results suggest that the visual
54 system is able to activate an array of circadian clock neurons (Li et al., 2018), e.g., it can
55 activate the small ventral lateral neurons (sLNvs), an important center for morning (M)
56 activity (Grima et al., 2004; Stoleru et al., 2004). Furthermore, the visual system increases
57 neuronal firing in the large LNvs (lLNvs), the arousal center within the circadian network
58 (Shang et al., 2008). The 5th sLNv and the NPF+ LNds, previously implicated as necessary
59 for evening (E) activity (Hermann et al., 2012; Rieger et al., 2006, 2009), also increase their
60 firing rates in response to visual system stimulation (Li et al., 2018). In addition, the visual
61 system activates several dorsal neurons (DN), which were recently implicated in connecting
62 the circadian clock to central brain sleep centers (Guo et al., 2018; Lamaze et al., 2018).
63 These data suggest that visual input is integrated into the clock network in a parallel fashion,
64 which contradicts a master-oscillator point of view (Li et al., 2018). The latter posits that
65 these are the pigment-dispersing factor (PDF)-expressing neurons (sLNvs and lLNvs), which
66 receive light input and release PDF upon illumination, thereby adjusting their downstream
67 target neurons to the LD cycle (Yoshii et al., 2016).

68 To investigate the impact of the visual input pathway at the behavioral and neuronal
69 level, we investigated fly behavior under long day conditions. Long days cause plastic
70 changes in fly behavior: In standard light-dark cycles of 12h light and 12h darkness (LD
71 12:12), flies show a bimodal activity pattern with a M anticipation peak around lights-on and
72 an E anticipation peak around lights-off; this results in a phase relationship of approximately
73 12h between the two peaks. Flies are able to adjust to longer photoperiods by delaying the E

74 peak, which reduces the potentially harmful impact of hot summer days (Rieger et al., 2003).
75 Previous experiments implicated the visual system in long day adaptation: Flies lacking the
76 compound eyes fail to appropriately adjust their peak timings (Rieger et al., 2003). It is still
77 unknown however which receptors and which neuronal pathways are involved in this
78 adjustment.

79 Here we show that R8 of the compound eyes is essential for long day adaptation.
80 These photoreceptor cells connect to the PDF-containing ILNvs and trigger the release of
81 this neuropeptide. Using a cell-specific CRISPR/Cas9 strategy, we demonstrate that light-
82 mediated PDF directly signals to the PDF receptor (PDFR) on E cells and hence delays E
83 activity. The data implicate a mammal-like structure of clock entrainment, with the visual
84 system activating PDF-expressing clock neurons. Our data further indicate a prominent shift
85 of PDF targets between LD and DD conditions as well as a more quantitative reorganization
86 of neuronal dominance within the clock network by changes in photoperiod.

87

88 **Material and Methods**

89 **Fly strains and rearing**

90 The following fly lines were used in this study: CantonS, *w¹¹¹⁸*, *cli^{eya}* (Bonini et al., 1993),
91 *ninaE⁵* (BL 3545), *rh3¹rh4¹* (Vasiliauskas et al., 2011), *rh5²;rh6¹* (Yamaguchi et al., 2008),
92 *rh5²;rh3¹rh4¹rh6¹* (Schlichting et al., 2014), *rh6-GAL4* (Sprecher and Desplan, 2008), *rh5-*
93 *GAL4* (Mazzoni et al., 2008), *rh3-GAL4* (Wernet et al., 2006), *rh4-GAL4* (Wernet et al.,
94 2006), UAS-*Kir2.1* (Baines et al., 2001), UAS-*HID* (BL 65403), *pdf(M)-GAL4* (Renn et al.,
95 1999), *pdf⁰¹* (Renn et al., 1999), UAS-*pdf-RNAi* (BL 25802), UAS-*pdf* (Renn et al., 1999),
96 UAS-*dcr2* (BL 24646), *R6-GAL4* (Helfrich-Förster et al., 2007), *c929-GAL4* (Hewes et al.,
97 2003), UAS-*DenMark* UAS-*syt.eGFP* (BL 33065), *clk856-GAL4* (Gummadova et al., 2009),
98 *mai179-GAL4* (Grima et al., 2004), *Spl-E-cell-GAL4* (Guo et al., 2017), *han⁵³⁰⁴*;UAS-*pdfr*
99 (Hyun et al., 2005; Mertens et al., 2005), UAS-*Cas9.P2* (BL 58986),
100 *w;CyO/Sco;MKRS/TM6B* (BL 3703). All flies were raised on standard cornmeal medium in
101 LD12:12 at 25 degrees.

102

103 **Behavior recording and analysis**

104 Single 2-6 days old male flies were transferred into glass tubes with food (1% agar and 4%
105 sucrose) on one end and a plug to close the tube on the other end. The glass tubes were placed
106 in *Drosophila* activity monitors (DAM) and a computer measured the number of light-beam
107 interruptions caused by the fly in one minute intervals. Behavior was either recorded in light
108 boxes within a climate controlled chamber or within incubators at constant temperature.

109 All flies were entrained for one week at LD 12:12. For photoreceptor mutants, flies
110 were exposed to either LD 14:10 or LD 16:8 in week 2 and either to LD 18:6 or LD 20:4 in
111 week 3. To investigate clock neuron interactions, flies were subjected to LD 20:4 after
112 entrainment in LD 12:12 for one week. To determine free-running behavior, we entrained

113 flies in LD 12:12 for at least 5 days and transferred them into constant darkness (DD) for at
114 least 7 days.

115 Behavior analysis was performed as described in (Schlichting and Helfrich-Förster,
116 2015). We first generated actograms using ActogramJ (Schmid et al., 2011) and calculated
117 average activity profiles out of the last 4 days of each light condition to allow for proper
118 entrainment. We then generated single-fly average days and determined the timing of M and
119 E peaks manually. Boxplots of single-fly values were generated to show the timing and the
120 distribution of the data. Free-running periods were determined using χ^2 analysis. Statistical
121 analysis was performed using two-way ANOVA (StataSE 15), one-way ANOVA followed
122 by post-hoc Tukey comparison (astata) or student's t-test (Excel).

123

124 **Fly line generation**

125 We generated a UAS-*PDFRg* fly line following the protocol of (Port and Bullock, 2016). In
126 short, we digested the vector pCFD6 (addgene #73915) with BbsI. We PCR amplified two
127 fragments carrying three independent guides for PDFR using Q5-polymerase (New England
128 BioLabs, NEB) and performed a Gibson assembly (NEB). Positive clones were sent for
129 injection to Rainbow Transgenic Flies (Camarillo, CA, USA) and inserted into the attP1
130 landing site on the second chromosome (BL 8621). W+ flies were balanced using BL3703
131 and kept as stable stocks above CyO. The following guides were used:

132 Guide 1: TCGAACATTCTCGACTGCGG

133 Guide 2: TGCTGGCCACCCACTCCGGC

134 Guide 3: CCTACATAGACATTGCCAGG

135

136

137

138 **Immunohistochemistry**

139 Brain staining: 2-6 days old male flies were fixed for 2h 45 min in 4% paraformaldehyde
140 (PFA) in phosphate-buffered saline including 0.5% Triton X (PBST) at room temperature
141 (RT). After rinsing 5x 10 min each with PBST, we dissected the brains and blocked with 5%
142 normal goat serum (NGS) in PBST. We applied primary antibodies overnight at RT. The
143 following antibodies were used: anti-PDF (1:1000, C7, Developmental Studies Hybridoma
144 Bank (DSHB)), anti-GFP (1:1500, abcam, ab13970), anti-dsRed (1:1000, Living Colors
145 DsRed Polyclonal Antibody, Takara). After rinsing 5x 10 min each in PBST, we applied
146 secondary antibodies (Invitrogen, 1:200 dilution) for 3h at RT. After washing 5x 10 min each
147 in PBST, brains were mounted on glass slides using Vectashield (VECTOR
148 LABORATORIES INC., Burlingame, CA, USA) mounting medium.

149 Retina staining: 2-6 days old male flies were fixed for 2h 30 min in 4% PFA in PBST at RT.
150 After washing 5x 10 min each with PBST, retinas were dissected in PBST and blocked in 5%
151 NGS in PBST for 1h at RT. Primary antibodies were applied for 2 nights at RT: anti-Rh1
152 (1:30, 4C5 DSHB), anti-Rh6 (1:2000, provided by C. Desplan, (Tahayato et al., 2003)), anti-
153 chaoptin (1:50, 24B10 DSHB) and anti-GFP (1:1500, abcam, ab13970). After rinsing 5x 10
154 min each in PBST, we applied secondary antibodies (Invitrogen, 1:200 dilution) for 3h at RT.
155 After washing 5x 10min each in PBST, retinas were mounted on glass slides using
156 Vectashield (VECTOR LABORATORIES INC., Burlingame, CA, USA) mounting medium.

157 Imaging: All images were obtained using either a Leica SPE or a Leica SP5 confocal
158 microscope. All brains/retinas were scanned using sections of 2 um thickness. Contrast and
159 brightness were adjusted using FIJI and Photoshop CS5 extended.

160

161

162

163 **Expansion Microscopy**

164 For expansion microscopy we applied the Pro-ExM protocol described in (Chen et al., 2015)
165 as modified in (Guo et al., 2018). In short, after applying the regular IHC protocol described
166 above, brains were transferred into the anchoring solution (Acryloyl X-SE, Life technologies
167 A20770, 1:100 in PBS) for 24h. We rinsed the brains 3x 10 min each in PBS, before the
168 gelling solution was added. We incubated the brains for 45 min on ice before transferring
169 them into the gel chamber, in which they were incubated at 37°C for 2h. After the gel
170 solidified, we trimmed away the excess gel material and applied the digestion buffer
171 (ProteinaseK, 1:100 in PBS) for 24h. Subsequently, we washed the brains 3x 20 min each in
172 ddH₂O and placed the brains on a glass bottom culture dish (MatTek Corp, P35GC-0-14-C)
173 with H₂O. We generated the brain images using the Zeiss LSM 880 confocal microscope
174 using z-stacks of 1 μ m. Image acquisition was performed using FIJI.

175

176

177

178

179 **Results**

180 **The compound eyes are essential for long day adaptation**

181 The locomotor activity of flies is controlled by their clock neuron network, which causes a
182 bimodal pattern. In wild type (WT) flies (CantonS) under standard LD 12:12 conditions, the
183 M peak of activity coincides with lights-on and the E peak with lights-off, respectively (Fig.
184 1A). In long photoperiods, the phase relationship between M and E peak increases showing
185 plasticity in clock-controlled behavior (Fig. 1A and 1D) (Rieger et al., 2003). The M peak
186 does not diverge from lights-on (Fig. 1B), whereas the E peak delays with increasing
187 photoperiod (Fig. 1C), demonstrating that a delay of E activity is responsible for the
188 enhanced phase relationship of the peaks (Fig. 1D). Notably, the E peak does not follow
189 lights-off under all light conditions: Whereas it coincides with lights-off at LD 12:12 and LD
190 14:10, it occurs during the light phase at even longer photoperiods, resulting in a maximal
191 phase relationship of 16.4 ± 0.3 h. Given that the E peak is the dominant factor for defining
192 the phase relationship and the M peak is also less pronounced in some of the mutants (Fig.
193 1G), we focus on E peak timing as a surrogate for phase.

194 To investigate the effect of the compound eyes on long day adaptation, we used *cli^{eya}*
195 mutants lacking the compound eyes but retaining ocelli and Hofbauer-Buchner-eyelets
196 (Schlichting et al., 2014). Even in LD12:12, the E peak is uncoupled from lights-off and is
197 significantly advanced compared to WT flies (Fig. 1E and 1G). Even though eyeless flies
198 adjust their E peak to long photoperiods (Fig. 1E and 1G), they fail to delay like WT flies,
199 resulting in an approximately 1.5h maximally advanced E peak timing under LD20:4. We
200 calculated Δ E-peak between CantonS and *cli^{eya}* mutants and found that this difference also
201 depends on photoperiod: The longer the photoperiod, the bigger the difference between
202 CantonS and *cli^{eya}*, resulting in a maximal difference in LD20:4 (Fig. 1F). Therefore, we use

203 this extreme photoperiod in the rest of this study to further investigate eye-mediated long day
204 adaptation.

205

206 **Receptor cell 8 is responsible for *eyes absent* phenotype**

207 The compound eyes are comprised of approximately 800 ommatidia. Each ommatidium
208 contains 8 photoreceptor cells (Rs) with R1-6 located in the periphery and spanning the
209 whole depth of the ommatidium. In the center, R7 is situated in the distal part of the
210 ommatidium right above R8. Besides the anatomical location, these cells express different
211 photopigments in a well-defined pattern: R1-6 express Rhodopsin 1 (Rh1), R7 express Rh3
212 and/or Rh4 and R8 express either Rh5 or Rh6 (Rister et al., 2013). To distinguish the
213 contribution of outer versus inner receptor cells, we compared the behavior of *ninaE*⁵ (no
214 Rh1) and *rh5*²;*rh3*¹*rh4*¹*rh6*¹ flies. *NinaE* flies show no difference in E peak timing in LD 20:4
215 compared to CantonS, *rh5*²;*rh3*¹*rh4*¹*rh6*¹ mutants in contrast show a significantly advanced E
216 peak, comparable to flies lacking the whole compound eyes (Fig. 2A and 2B). These data
217 suggest that the inner photoreceptors are necessary to mediate long day adaptation.

218 To narrow down the phenotype to a specific inner receptor cell, we monitored the
219 behavior of *rh3*¹*rh4*¹ mutants eliminating R7 function and *rh5*²;*rh6*¹ mutants eliminating R8
220 function. *rh3*¹*rh4*¹ mutants behave similar to WT, whereas *rh5*²;*rh6*¹ mutants show an
221 advanced E peak in LD 20:4 indistinguishable from *rh5*²;*rh3*¹*rh4*¹*rh6*¹ quadruple mutants
222 (Fig. 2A and 2B). This suggests that the rhodopsins of R8 are necessary for WT E peak
223 timing under long photoperiods.

224 To further confirm the importance of R8 we combined *rh5-GAL4* and *rh6-GAL4* and
225 either silenced these two cell types using UAS-*Kir2.1* or ablated the cells using UAS-*HID*.
226 Immunohistochemistry shows strong specificity of the combined GAL4 lines and a
227 successful ablation of R8 without affecting other photoreceptors in the HID experiment

228 (Suppl. Fig. 1). As with the rhodopsin mutants, ablating or silencing R8 caused a 1.5 hour
229 advance in E activity, confirming an important role for this photoreceptor cell. We further
230 silenced or ablated R7 using a combination of *rh3-GAL4* and *rh4-GAL4*. As expected, there is
231 no effect on E peak timing, confirming the rhodopsin mutant approach data (Suppl. Fig. 2).

232 As an early E peak might represent a “fast” clock, we monitored the behavior of all
233 mutants in constant darkness (Table 1). We found no correlation between E peak timing and
234 period length, suggesting the long photoperiod phenotype is a true entrainment phenomenon.
235

236 **PDF in ILNvs is necessary and sufficient for proper E peak timing**

237 The terminals of R8 directly innervate the medulla, the visual center of the fly, where they sit
238 in close proximity to ILNv arborizations (Schlichting et al., 2016). GRASP experiments
239 between R8 and PDF positive neurons did not give a signal in the medulla, suggesting no
240 direct interaction between the compound eyes and the clock (data not shown). However,
241 electrophysiological data suggest that the visual system activates the PDF expressing ventro-
242 lateral neurons (among others) upon light stimulation (Li et al., 2018; Muraro and Ceriani,
243 2015). To address the importance of the PDF neurons for long day entrainment, we silenced
244 these cells using *UAS-Kir2.1* (Fig. 3A). Silencing the PDF neurons significantly advances the
245 E peak timing by approximately 1.5h, recapitulating the *cli^{eya}* phenotype (Fig. 3B).

246 PDF is the major neuropeptide of the *Drosophila* clock and is essential to synchronize
247 the different clock neuron clusters with each other (Helfrich-Förster et al., 2007). Previous
248 work showed that PDF from ILNvs is necessary to adapt fly behavior to LD 16:8 (Schlichting
249 et al., 2016). We asked, whether PDF from these neurons is also necessary for proper E Peak
250 timing under even longer days (LD 20:4) and investigated the behavior of *pdf⁰¹* flies (Yoshii
251 et al., 2009) (Fig. 3B and 3C). As with the *pdf>Kir* experiment, *pdf⁰¹* flies show an advanced
252 E peak, indicating that PDF signalling to its downstream target neurons is necessary for the

253 delay of the E peak in long photoperiods. To determine, which group of PDF neurons is
254 essential for this behavior, we knocked down PDF using RNAi. PDF knockdown in all PDF-
255 positive cells (sLNvs and ILNvs) results as expected in an advanced E peak compared to both
256 controls (Fig. 3B and 3C). Knockdown only in sLNv using *R6-GAL4* does not advance the
257 timing of the E peak. In contrast, knockdown in ILNvs using *c929-GAL4* completely
258 reproduces universal PDF knockdown (Fig. 3B and 3C) indicating that PDF from the ILNvs
259 is necessary for proper E peak timing under long day conditions.

260 To address if ILNv-derived PDF is also sufficient for WT behavior, we expressed
261 PDF in the ILNvs using *c929-GAL4* in the *pdf⁰¹* null mutant background (Fig. 3E). The
262 timing of the E peak was delayed by approximately 1.5h (Fig. 3F), which recapitulates the
263 WT phenotype. The two approaches taken together indicate that PDF from the ILNvs is
264 necessary and sufficient for WT behavior under long photoperiod conditions (Menegazzi et
265 al., 2017).

266

267 **E cells show extensive arborizations in the accessory medulla**

268 Previous experiments implicate the 5th sLNv and three CRY-positive neurons in
269 driving/timing the E peak, the evening bout of activity (Grima et al., 2004; Stoleru et al.,
270 2004). These neurons broadly innervate the dorsal part of the brain where they receive
271 glutamatergic input (Guo et al., 2016). They also send fibers into the area of the accessory
272 medulla of the fly brain, the location of the PDF cell bodies and an important pacemaker
273 center in many other insect species (Helfrich-Förster et al., 2007; Schubert et al., 2018).

274 To determine, whether ILNv-derived PDF could communicate with the E cells in that
275 area, we expressed synaptic markers in the E cells. This was done using a recently identified
276 split-GAL4 line, which expresses only in the three CRY+ LNds and the 5th sLNv (Guo et al.,
277 2017). Whole brain imaging reproduces the previously published projection pattern, showing

278 strong synaptic marker staining in the dorsal brain (Fig. 4A-4D). In the accessory medulla
279 however, we found only weak staining of dendritic and axonal markers. To further illuminate
280 the nature of these E cell fibers, we employed expansion microscopy and focused on this
281 area. The much better resolution indicates that the accessory medulla is indeed densely
282 innervated by E cell fibers, both synaptic as well as dendritic markers (Fig. 4E-4H). It is
283 therefore a likely output as well input region of E cells. The accessory medulla more
284 generally seems to serve as a region of communication between clock neurons, e.g., the
285 ILNvs probably communicate there with the sLNvs via PDF (Choi et al., 2012).

286

287 **PDFR in E cells is necessary and sufficient for proper E peak timing**

288 Loss of PDF or its receptor PDFR (*han*⁵³⁰⁴ mutant) causes prominent effects on LD 12:12 and
289 DD behavior: mutant flies show a reduced M anticipation and an early E peak in LD as well
290 as elevated arrhythmicity and a short period phenotype in DD (Hyun et al., 2005; Mertens et
291 al., 2005; Renn et al., 1999). To address the importance of PDFR+ E cells for the long day
292 phenotype, we employed a cell-specific CRISPR/Cas9 strategy with the GAL4/UAS system.
293 We generated an *UAS-PDFRg* line, expressing three independent guides, each targeting the
294 CDS of the *pdf* gene. To verify the efficiency of this strategy, we expressed *PDFRg* and
295 *Cas9* in most of the clock neuron network using *clk856-GAL4*. It reproduced the *han*⁵³⁰⁴
296 mutant phenotype: flies show a low M anticipation index and an early E peak in LD12:12,
297 and only 37% of the flies are rhythmic with a short period of 22.7 hours in DD (Suppl. Fig.
298 3).

299 We then applied the same strategy to long photoperiods. Knocking out PDFR in most
300 clock cells using *clk856-GAL4* reproduced the early E peak phenotype seen in *eyes absent*
301 and *pdf*⁰¹ flies, further indicating that PDF signaling within the clock network is essential for
302 long day adaptation (Fig. 5A and 5B). Knocking out PDFR in E cells using *Mai179-GAL4*

303 reproduced the same behavioral phenotype, i.e., an early E peak under long day conditions
304 (Fig. 5A and 5B). Remarkably, DD behavior was unaffected: 73% of flies were rhythmic
305 with a period of 23.8 ± 0.2 h, indicating that E cell PDFR is only required in LD conditions
306 (Suppl. Fig. 4).

307 Due to a lack of specific driver lines, a previous study implicated E cell PDFR in long day
308 entrainment based on an overlap analysis of much broader driver lines or driver lines with
309 ectopic expression (Schlichting et al., 2016). In contrast, GAL4 lines used here can directly
310 assign E cells to this function. To this end, we rescued PDFR in most of the clock neuron
311 network which delayed the timing of the E peak to WT levels (Fig. 5C and 5D). Rescue of
312 PDFR only in the three CRY+ LNds and the 5th sLNv also delayed the E peak compared to
313 both controls, showing that PDFR in the E cells is indeed sufficient to rescue the E peak
314 timing under long days.

315 **Discussion**

316 The circadian clock is able to entrain to the changes of day and night, with light being the
317 most important zeitgeber. The adaptation to summer-like days is especially important for
318 insects, as they are prone to predator visibility and even more importantly desiccation.
319 Therefore, the circadian clock has to be plastic and be able to adjust behavior to changing
320 environments. Here we show that *Drosophila* adjusts its behavior to long photoperiods, by
321 delaying its E peak as reported previously (Rieger et al., 2003). This delay allows the animal
322 to reduce its activity during the unfavorable midday, when temperatures are highest. Most
323 interestingly, this phenotype is easily visible even without temperature changes, underscoring
324 the importance of light as the major entrainment cue.

325 A central finding is that flies lacking the compound eyes show an entrainment deficit,
326 i.e., they have an advanced E peak under long day conditions. Using rhodopsin mutants and
327 by manipulating specific photoreceptors using the GAL4/UAS-system, only R8 is essential
328 for summer day adaptation. Interestingly, R8 was already implicated in the adaptation to
329 nature-like light conditions (Schlichting et al., 2014, 2015).

330 ILNv arbors in the optic lobe are in close proximity to R8 termini, (Schlichting et al.,
331 2016), where they most-likely interact via cholinergic interneurons. This interaction results in
332 a change of neuronal bursting behavior and hence neuropeptide release (Barber et al., 2016;
333 Muraro and Ceriani, 2015). Indeed, we show here that release of PDF from the ILNvs is
334 necessary and sufficient for proper long day adaptation.

335 These results are surprising given a recently published study on photic entrainment
336 (Li et al., 2018). It shows that the visual system can activate a broad spectrum of lateral and
337 dorsal neurons; they include sLNvs, ILNvs, ITP+ LNds and DN2s among others. Ablation of
338 PDF neurons left the other neurons responsive to visual input, suggesting a parallel model for
339 clock synchronization, i.e., information from the visual system can be directly transferred to

340 independent classes of clock neurons rather than only via PDF. Nonetheless, we show here
341 that PDF signaling from the ILNvs to the LNds is essential for proper long day adaptation,
342 suggesting that direct transfer of light information to other clock neurons serves other light-
343 mediated functions.

344 PDF stimulates different adenylate-cyclases and increases cAMP, which leads to the
345 stabilization of PER and consequently a longer period or phase delay (Duvall and Taghert,
346 2012; Li et al., 2014). Therefore, one view is that removing the compound eyes decreases
347 PDF release from the ILNvs and phase-advances the molecular clock in downstream target
348 neurons like the LNds. This newly discovered “visual system to LNd pathway” might also
349 enhance CRY-mediated photoentrainment: CRY was shown to activate neurons upon
350 stimulation (Fogle et al., 2011), similar to the newly identified light activation of clock
351 neuron pathway (Li et al., 2018). Additional activation of the E cells could therefore
352 contribute to the kinetics of TIM degradation, which was recently shown to be important for
353 the phase advance of E activity under long day conditions (Kistenpfennig et al., 2018).

354 An intriguing inference of this work is that the principal targets of PDF must change
355 with the environmental conditions. Previous work established the sLNvs as essential for DD
356 rhythmicity (Grima et al., 2004; Stoleru et al., 2004), and recent work shows that these
357 neurons are tightly coupled to the dorsal clock neurons in DD: speeding up the PDF neurons
358 forced the DN1s to follow the short period of the sLNvs (Chatterjee et al., 2018). In LD
359 however, this connection is much weaker, and our cell-type specific CRISPR/Cas9 knockout
360 strategy shows that it is the PDF expressing ILNvs communicate with the LNd neurons
361 (Chatterjee et al., 2018). Our data show that the ILNv to LNd connection is important in LD
362 conditions but does not affect DD behavior.

363 Importantly, our data not only indicate a qualitative shift of PDF targets between DD
364 and LD but also suggest a quantitative shift of dominance depending on photoperiod or the

365 time of light exposure. In DD, the sLNvs are necessary for rhythmic behavior and show
366 robust cycling in PER oscillations, whereas the lLNvs lose PER rhythms as early as the
367 second day of DD. In equinox conditions, both groups may be relevant (Schlichting et al.,
368 2019): PDF from either the sLNvs or lLNvs is sufficient for WT behavior, and only
369 knockdown in both sets of neurons is able to reproduce the *pdf⁰¹* mutant phenotype (Shafer
370 and Taghert, 2009). In long photoperiods however, PDF from the lLNvs is necessary and
371 sufficient for proper entrainment, whereas the sLNvs do not contribute to E peak timing
372 (Schlichting et al., 2016). Our data therefore point to a profound circuit switch in response to
373 photoperiod, analogous to the neurotransmitter switching that occurs in the mammalian
374 paraventricular nucleus in response to long photoperiods (Meng et al., 2018).

375 A similar circuit reorganization might also occur in the principal mammalian brain
376 clock neuron location, the suprachiasmatic nucleus (SCN). We know that light information
377 from the visual system is transferred to cells in the ventral part of the SCN, which expresses
378 VIP (Abrahamson and Moore, 2001). VIP functions similarly to *Drosophila* PDF and is not
379 only important for communication between different parts of the SCN (Aton et al., 2005) but
380 also essential for seasonal encoding. This is because VIP knockout mice show no change in
381 peak width as measured by *in vivo* electrophysiological recordings in response to entrainment
382 to different photoperiods (Lucassen et al., 2012). This suggests that VIP is not only involved
383 in relaying light information beyond the ventral SCN but also in the response to light duration
384 as shown here for PDF in *Drosophila*. It will be interesting to see if different VIP-expressing
385 SCN neurons are involved in this response.

386 **Competing Interests:**

387 The authors declare no competing interests.

388

389 **Author Contributions:**

390 Conceptualization M.S., C.H.F. and M.R.; Methodology M.S., C.H.F. and M.R.;

391 Investigation M.S., P.W., M.D., P.M. and E.D.B.; Visualization M.S., M.D. and P.W.;

392 Writing - Original Draft M.S. and M.R.; Funding Acquisition M.S., C.H.F. and M.R.;

393 Resources C.H.F. and M.R.

394

395 **Acknowledgements**

396 We would like to thank Dr. Leslie Griffith and Dr. Katharine Abruzzi for discussions and

397 comments on the manuscript. Also, we are thankful to Dr. Claude Desplan, Dr. Martin

398 Heisenberg and Dr. Dragana Rogulja for providing fly lines and antibodies. Stocks obtained

399 from the Bloomington *Drosophila* Stock Center (NIH P40OD018537) were used in this

400 study. This work was supported by the German Research Foundation (DFG) Collaborative

401 Research Center (SFB1047 Project A2) and the Howard Hughes Medical Institute (HHMI).

402 M.S. was sponsored by a DFG research fellowship (SCHL2135 1/1).

403

404 **Figure Legends**

405 **Figure 1** The compound eyes contribute to long photoperiod entrainment. **A** Average activity
406 profiles of CantonS flies from LD 12:12 (top) to LD 20:4 (bottom). Daylight period increases
407 by 2 hours per light condition. Flies show a bimodal activity pattern at every light condition
408 with a broader E peak at longer photoperiods. **B** Timing of Morning (M) activity peak of
409 CantonS flies at equinox and long day conditions. The M peak is tightly coupled to lights-on.
410 It shows a tendency to delay with increasing day-length, which is not significant
411 ($F_{(4,146)}=1.8064$, $p=0.1307$). **C** Timing of Evening (E) activity peak of CantonS flies at
412 equinox and long day conditions. Timing of the E peak delays with increasing day length, but
413 does not follow lights off ($F_{(4,146)}=177.09$, $p<0.001$). **D** Phase-relationship of M peak to E
414 peak in CantonS at equinox and long day conditions. Due to the delay of the E peak timing,
415 also the phase relationship increases with increasing daytime ($F_{(4,146)}=139.49$, $p<0.001$). **E**
416 Timing of E activity peak of *cli^{eya}* flies at equinox and long day conditions. One-way
417 ANOVA shows that *cli^{eya}* flies delay their E peak timing with increasing daytime
418 ($F_{(4,137)}=72.25$, $p<0.001$). Two-way ANOVA shows a significant difference between CantonS
419 and *cli^{eya}* flies ($F_{(1,283)}=149.23$, $p<0.001$) and a significant interaction between genotype and
420 photoperiod, suggesting differential regulation of long day adaptation in the two genotypes
421 ($F_{(1,283)}=3.85$, $p=0.0046$). **F** Difference of E peak timing between CantonS and *cli^{eya}* flies
422 depending on day length. One-way ANOVA reveals a significant difference between the two
423 genotypes, which is in agreement with the interaction of genotype and photoperiod described
424 in E ($F_{(4,137)}=3.2766$, $p=0.0134$). The biggest difference between the genotypes was found in
425 LD 20:4. **G** Average activity profiles of *cli^{eya}* flies from LD 12:12 (top) to LD 20:4 (bottom).
426 Daylight period increases by 2 hours per light condition. *cli^{eya}* flies show a bimodal pattern in
427 LD 12:12 which turns into unimodal behavior under long days with an early E peak timing.

428 **Figure 2** R8 is necessary for long day adaptation. **A** Average activity profiles of
429 photoreceptor mutants recorded in LD 20:4. All genotypes show a bimodal activity pattern
430 with a M peak around lights on and an E peak uncoupled from lights-off. **B** Timing of the E
431 peak in CantonS and all photoreceptor mutants was investigated. One-way ANOVA reveals
432 significant differences between the different genotypes ($F_{(5,161)}=62.6166$, $p<0.001$). Post-Hoc
433 Tukey comparison shows a significantly advanced E peak in *cli^{eya}* mutants compared to
434 CantonS ($p=0.001$). Similar advances are seen in flies lacking photoreception in both inner
435 receptor cells (*rh5²;rh3¹rh4¹rh6¹*, $p=0.001$) and flies lacking photoreception only in R8
436 (*rh5²;rh6¹*, $p=0.001$). There was no difference between *cli^{eya}* and *rh5²;rh6¹* mutants
437 ($p=0.899$), suggesting a prominent role of R8 in long day adaptation. Flies lacking
438 photoreception in R1-6 (*ninaE⁵*) show no difference to CantonS ($p=0.776$), whereas there is a
439 slight but significant delay in flies lacking photoreception in R7 (*rh3¹rh4¹*, $p=0.001$). **C**
440 Timing of the E peak in flies with silenced or ablated R8. One-way ANOVA reveals
441 significant differences between the different genotypes ($F_{(4,150)}=25.45$, $p<0.001$). Post-Hoc
442 Tukey comparison shows a significantly advanced E peak in flies with silenced R8 ($p=0.001$
443 for both controls) and flies with ablated R8 ($p=0.001$ for both controls). There were neither
444 significant differences between the controls ($p>0.775$) nor between the two experimental
445 lines ($p=0.8926$) demonstrating an important role of R8 for long day adaptation. **D** Average
446 activity profiles of flies with ablated (left) or silenced (right) R8 recorded in LD 20:4. All
447 genotypes show a bimodal activity pattern with a M peak around lights on and an E peak
448 uncoupled from lights-off.

449

450 **Figure 3** PDF release from the ILNvs is essential for long day adaptation **A** Average activity
451 profiles of control flies (*UAS-Kir*, left) and flies with silenced PDF neurons (*pdf>Kir*, right)
452 in LD 20:4. Flies show a bimodal activity pattern. The timing of the E peak is significantly

453 advanced in *pdf>Kir* flies. **B** Timing of the E peak in flies with silenced PDF neurons
454 including controls in LD 20:4. One-way ANOVA reveals a significant difference between the
455 genotypes ($F_{(2,89)}=70.1449$, $p<0.001$). Post-hoc Tukey test shows a significantly advanced E
456 peak in *pdf>Kir* compared to both controls ($p=0.001$ for both). There was no significant
457 difference within control groups ($p=0.758$). **C** Timing of the E peak in flies with altered PDF
458 expression including controls in LD 20:4. One-way ANOVA reveals a significant difference
459 between the genotypes ($F_{(8,178)}=28.607$, $p<0.001$). Post-hoc Tukey analysis show that the
460 timing of the E peak is significantly advanced in *pdf⁰¹* compared to CantonS flies ($p=0.001$).
461 Similarly, knockdown of PDF using RNAi in both, the sLNvs and ILNvs significantly
462 advanced E peak timing ($p=0.001$ for both controls). Knockdown of PDF in the sLNvs using
463 *R6-GAL4* had no effect on E peak timing ($p=0.899$ for both controls), whereas the
464 knockdown in ILNvs using *c929-GAL4* significantly advanced E peak timing ($p=0.001$ for
465 both controls). There is no difference between *pdf-GAL4* and *c929-GAL4* mediated
466 knockdown ($p=0.899$) indicating PDF from the ILNvs is necessary for WT behavior. **D**
467 Average activity profiles of *pdf⁰¹* (top left), PDF-knockdown in all lateral neurons (top right),
468 PDF knockdown in sLNvs (bottom left) and PDF knockdown in ILNvs (bottom right) in LD
469 20:4. Flies show a bimodal activity pattern. The timing of the E peak is significantly
470 advanced in flies lacking PDF at least in the ILNvs. **E** Average activity profile of PDF rescue
471 in ILNvs in LD 20:4. Rescue of PDF only in ILNvs restores WT behavior. **F** E peak timing of
472 ILNv specific PDF rescue and control. Student's t-test shows a significant delay of E peak
473 timing ($p<0.001$) when PDF is rescued in the ILNvs.

474

475 **Figure 4** Anatomy of E-cell arborizations in the brain of *Drosophila*. **A-D** Maximum
476 projection of *Spl-E-GAL4>Syt-GFP Den-RFP* flies using regular IHC. **A** Synaptic markers
477 (green) are predominantly present in the dorsal part of the brain. **B** Dendritic markers (red)

478 are more prominent in the accessory medulla. **C** PDF staining (magenta) labels ILNv and
479 sLNv neurons and their projections. **D** Composite of all channels. **E-G** Projections of *Spl-E-*
480 *GALA>Syt-GFP Den-RFP* flies in the accessory medulla (aMe) using expansion microscopy.
481 The aMe is densely innervated by E-cells, which express synaptic (green, **E**) and dendritic
482 (red, **F**) markers in close vicinity of PDF neuron fibers (magenta, **G**). **H** Composite of all
483 channels showing axonal-dendritic nature of E cell arborizations in the aMe.

484

485 **Figure 5** PDFR in E cells is necessary and sufficient for proper E peak timing in LD 20:4. **A**
486 Average activity profiles of *clk856>Cas9* control (top left), PDFR knockout in all clock
487 neurons (top right), *mai179-GALA>Cas9* control (bottom left) and PDFR knockout in E-cells
488 using *mai179-GALA* (bottom right) in LD 20:4. Flies show a bimodal activity pattern with a
489 M peak around lights-on and an E-peak uncoupled from lights-off. **B** Timing of the E peak in
490 PDFR knockout flies including controls in LD 20:4. One-way ANOVA reveals a significant
491 difference between the genotypes ($F_{(4,131)}=23.945$, $p<0.001$). Post-hoc Tukey test shows a
492 significantly advanced E peak in PDFR knockout in all clock cells compared to both controls
493 ($p=0.001$ for both). Similarly, knockout of PDFR using *mai179-GALA* advanced the E peak
494 timing compared to both controls ($p=0.001$ for both). There was no significant difference
495 between the two knockout strains ($p=0.899$) showing that PDFR in E cells is necessary for
496 proper E peak timing. **C** Timing of the E peak in PDFR rescue flies including controls in LD
497 20:4. One-way ANOVA reveals a significant difference between the genotypes
498 ($F_{(4,125)}=43.358$, $p<0.001$). Post-hoc Tukey test shows a significantly delayed E peak in PDFR
499 rescue in all clock cells compared to both controls ($p=0.001$ for both). Similarly, rescue of
500 PDFR using *E-cell-Spl-GALA* delayed the E peak timing compared to both controls ($p=0.001$
501 for both). **D** Average activity profiles of *han⁵³⁰⁴;clk856-GALA* control (top left), PDFR rescue
502 in all clock neurons (top right), *han⁵³⁰⁴;E-cell-Spl-GALA* control (bottom left) and PDFR

503 rescue in E-cells using *E-cell-Spl-GAL4* (bottom right) in LD 20:4. Flies show a bimodal
504 activity pattern with a M peak around lights-on and an E-peak uncoupled from lights-off.

505

506 **Suppl Figure 1** *rh5 rh6-GAL4* combination expresses in all R8s and is able to ablate
507 photoreceptor cells. **A** *rh5rh6>mGFP* stained with anti-GFP (green), anti-Rh1 (red) and anti-
508 Rh6 (magenta). Cross-section through proximal part of the retina shows GFP expression in
509 all inner photoreceptors, but no expression in R1-6. Longitudinal sections show specificity to
510 R8: GFP expression is found in the proximal but not the distal part of the retina. **B** anti-
511 Choptin staining of *rh5rh6>HID* (cyan). Choptin labels all rhabdomeres. Whereas WT
512 retinas show 7 rhabdomeres per cross section (R1-6 and either R7 or R8), *rh5rh6>HID* flies
513 have only R1-6 remaining, suggesting efficient ablation of R8 in this line. Notably, R1-6
514 structure seems unaffected.

515

516 **Suppl Figure 2** Ablation or silencing R7 has no effect on long day entrainment. **A** Average
517 activity profiles of *rh3rh4-GAL4* control (top left), *UAS-Kir2.1* control (middle panel, left),
518 *UAS-HID* control (lower panel, left) and flies with silenced R7 (middle panel, right) and flies
519 with ablated R7 (lower panel, right) in LD 20:4. Flies show a bimodal activity pattern with a
520 M peak around lights-on and an E-peak uncoupled from lights-off. **B** Timing of the E peak in
521 R7 silenced or R7 ablated flies including controls in LD 20:4. One-way ANOVA with post-
522 hoc Tukey test reveals no significant difference between the genotypes ($p>0.144$ for pairwise
523 comparisons).

524

525 **Suppl Figure 3** Expression of *PDFRg* and *Cas9* in all clock neurons reproduces *han*⁵³⁰⁴
526 mutant phenotype **A** Example actograms of flies entrained in LD 12:12 for 5 days (indicated
527 by yellow box) and released into constant darkness (DD). Flies either show rhythmic

528 behavior with short period in DD (left example) or arrhythmic behavior (right example). **B**
529 Average activity profiles of *clk856>Cas9* control (left), *clk856>Cas9 PDFRg* (middle) and
530 *UAS-PDFRg* control (right) in LD 12:12. Both controls show a bimodal activity pattern with
531 a M peak around lights-on and an E peak around lights-off. Experimental flies show reduced
532 M anticipation and an advanced E peak comparable to *han⁵³⁰⁴* mutant flies. **C** Percentage
533 rhythmic flies in DD. Both controls show a high percentage of rhythmicity (>90%), whereas
534 less than 40% of PDFR-KO flies remained rhythmic. **D** Free-running period in DD. The
535 period of PDFR-KO flies is about 1h shorter than both controls.

536

537 **Suppl Figure 4** Knockout of PDFR using *mai179-GAL4* has no effect on DD behavior **A**
538 Percentage rhythmic flies in DD. All genotypes show high percentage of rhythmicity (>90%).
539 **B** Free-running period in DD. There is no effect on period length.

540

541 **Table 1** Free-running behavior of WT flies and flies with manipulated visual system. All flies
542 show a period close to 24h.

	% rhythmic flies	period \pm SEM	power \pm SEM
<i>CantonS</i>	84	24.3 \pm 0.1	26.7 \pm 1.9
<i>cli^{eya}</i>	100	23.6 \pm 0.1	25.4 \pm 1.9
<i>ninaE</i>	100	23.9 \pm 0.1	44.2 \pm 1.6
<i>rh5²;rh3¹rh4¹rh6¹</i>	23	23.6 \pm 0.1	24.0 \pm 3.1
<i>rh3¹rh4¹</i>	83	23.5 \pm 0.1	25.2 \pm 1.2
<i>rh5²;rh6¹</i>	100	23.3 \pm 0.1	23.0 \pm 1.8
<i>UAS-HID</i>	100	23.9 \pm 0,1	50.7 \pm 2.6
<i>rh5 rh6>HID</i>	100	23.4 \pm 0.1	39.1 \pm 3.5
<i>rh5 rh6-GAL4</i>	100	23.3 \pm 0.1	47.6 \pm 1.8
<i>rh5 rh6>Kir</i>	100	23.3 \pm 0.1	39.6 \pm 1.9
<i>UAS-Kir</i>	100	23.6 \pm 0.1	28.1 \pm 2.0

543

544

545 **References:**

- 546 Abrahamson, E.E., and Moore, R.Y. (2001). Suprachiasmatic nucleus in the mouse: retinal
547 innervation, intrinsic organization and efferent projections. *Brain Res.* 916, 172–191.
- 548 Aton, S.J., Colwell, C.S., Harmar, A.J., Waschek, J., and Herzog, E.D. (2005). Vasoactive
549 intestinal polypeptide mediates circadian rhythmicity and synchrony in mammalian clock
550 neurons. *Nat. Neurosci.* 8, 476–483.
- 551 Baines, R.A., Uhler, J.P., Thompson, A., Sweeney, S.T., and Bate, M. (2001). Altered
552 electrical properties in *Drosophila* neurons developing without synaptic transmission. *J.*
553 *Neurosci.* 21, 1523–1531.
- 554 Barber, A.F., Erion, R., Holmes, T.C., and Sehgal, A. (2016). Circadian and feeding cues
555 integrate to drive rhythms of physiology in *Drosophila* insulin-producing cells. *Genes Dev.*
556 30, 2596–2606.
- 557 Berson, D.M., Dunn, F.A., and Takao, M. (2002). Phototransduction by retinal ganglion cells
558 that set the circadian clock. *Science* 295, 1070–1073.
- 559 Bonini, N.M., Leiserson, W.M., and Benzer, S. (1993). The eyes absent gene: genetic control
560 of cell survival and differentiation in the developing *Drosophila* eye. *Cell* 72, 379–395.
- 561 Chatterjee, A., Lamaze, A., De, J., Mena, W., Chélot, E., Martin, B., Hardin, P., Kadener, S.,
562 Emery, P., and Rouyer, F. (2018). Reconfiguration of a Multi-oscillator Network by Light in
563 the *Drosophila* Circadian Clock. *Curr. Biol.* 28, 2007–2017.e4.
- 564 Chen, F., Tillberg, P.W., and Boyden, E.S. (2015). Optical imaging. Expansion microscopy.
565 *Science* 347, 543–548.
- 566 Choi, C., Cao, G., Tanenhaus, A.K., McCarthy, E.V., Jung, M., Schleyer, W., Shang, Y.,
567 Rosbash, M., Yin, J.C.P., and Nitabach, M.N. (2012). Autoreceptor control of
568 peptide/neurotransmitter corelease from PDF neurons determines allocation of circadian
569 activity in *drosophila*. *Cell Rep.* 2, 332–344.
- 570 Czeisler, C.A., Duffy, J.F., Shanahan, T.L., Brown, E.N., Mitchell, J.F., Rimmer, D.W.,
571 Ronda, J.M., Silva, E.J., Allan, J.S., Emens, J.S., et al. (1999). Stability, precision, and near-
572 24-hour period of the human circadian pacemaker. *Science* 284, 2177–2181.
- 573 Dubowy, C., and Sehgal, A. (2017). Circadian Rhythms and Sleep in *Drosophila*
574 *melanogaster*. *Genetics* 205, 1373–1397.
- 575 Duvall, L.B., and Taghert, P.H. (2012). The circadian neuropeptide PDF signals
576 preferentially through a specific adenylate cyclase isoform AC3 in M pacemakers of
577 *Drosophila*. *PLoS Biol.* 10, e1001337.
- 578 Fogle, K.J., Parson, K.G., Dahm, N.A., and Holmes, T.C. (2011). CRYPTOCHROME is a
579 blue-light sensor that regulates neuronal firing rate. *Science* 331, 1409–1413.
- 580 Golombek, D.A., and Rosenstein, R.E. (2010). Physiology of Circadian Entrainment. *Physiol.*
581 *Rev.* 90, 1063–1102.

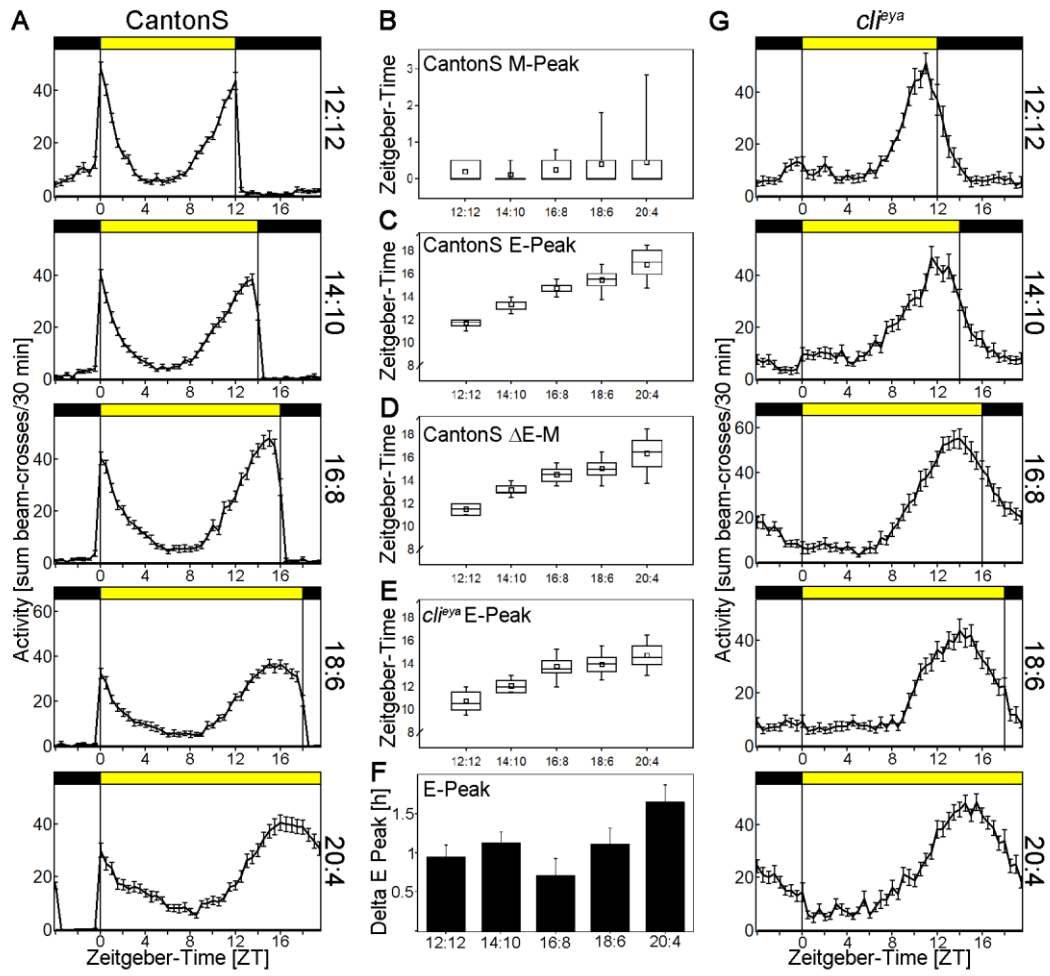
- 582 Grima, B., Chélot, E., Xia, R., and Rouyer, F. (2004). Morning and evening peaks of activity
583 rely on different clock neurons of the *Drosophila* brain. *Nature* 431, 869–873.
- 584 Gummadova, J.O., Coutts, G.A., and Glossop, N.R.J. (2009). Analysis of the *Drosophila*
585 Clock promoter reveals heterogeneity in expression between subgroups of central oscillator
586 cells and identifies a novel enhancer region. *J. Biol. Rhythms* 24, 353–367.
- 587 Guo, F., Yu, J., Jung, H.J., Abruzzi, K.C., Luo, W., Griffith, L.C., and Rosbash, M. (2016).
588 Circadian neuron feedback controls the *Drosophila* sleep--activity profile. *Nature* 536, 292–
589 297.
- 590 Guo, F., Chen, X., and Rosbash, M. (2017). Temporal calcium profiling of specific circadian
591 neurons in freely moving flies. *Proc. Natl. Acad. Sci. U. S. A.* 114, E8780–E8787.
- 592 Guo, F., Holla, M., Díaz, M.M., and Rosbash, M. (2018). A Circadian Output Circuit
593 Controls Sleep-Wake Arousal in *Drosophila*. *Neuron* 100, 624–635.e4.
- 594 Hardin, P.E. (2011). Molecular genetic analysis of circadian timekeeping in *Drosophila*. *Adv.*
595 *Genet.* 74, 141–173.
- 596 Hattar, S., Liao, H.W., Takao, M., Berson, D.M., and Yau, K.W. (2002). Melanopsin-
597 containing retinal ganglion cells: architecture, projections, and intrinsic photosensitivity.
598 *Science* 295, 1065–1070.
- 599 Helfrich-Förster, C., Yoshii, T., Wülbeck, C., Grieshaber, E., Rieger, D., Bachleitner, W.,
600 Cusumano, P., and Rouyer, F. (2007). The lateral and dorsal neurons of *Drosophila*
601 *melanogaster*: new insights about their morphology and function. *Cold Spring Harb. Symp.*
602 *Quant. Biol.* 72, 517–525.
- 603 Hermann, C., Yoshii, T., Dusik, V., and Helfrich-Förster, C. (2012). Neuropeptide F
604 immunoreactive clock neurons modify evening locomotor activity and free-running period in
605 *Drosophila melanogaster*. *J. Comp. Neurol.* 520, 970–987.
- 606 Hewes, R.S., Park, D., Gauthier, S.A., Schaefer, A.M., and Taghert, P.H. (2003). The bHLH
607 protein Dimmed controls neuroendocrine cell differentiation in *Drosophila*. *Development*
608 130, 1771–1781.
- 609 Hofbauer, A., and Buchner, E. (1989). Does *Drosophila* have seven eyes?
610 *Naturwissenschaften* 76, 335–336.
- 611 Hyun, S., Lee, Y., Hong, S.-T., Bang, S., Paik, D., Kang, J., Shin, J., Lee, J., Jeon, K.,
612 Hwang, S., et al. (2005). *Drosophila* GPCR *Han* is a receptor for the circadian clock
613 neuropeptide PDF. *Neuron* 48, 267–278.
- 614 Kistenpfennig, C., Nakayama, M., Nihara, R., Tomioka, K., Helfrich-Förster, C., and Yoshii,
615 T. (2018). A Tug-of-War between Cryptochrome and the Visual System Allows the
616 Adaptation of Evening Activity to Long Photoperiods in *Drosophila melanogaster*. *J. Biol.*
617 *Rhythms* 33, 24–34.
- 618 Lamaze, A., Krätschmer, P., Chen, K.-F., Lowe, S., and Jepson, J.E.C. (2018). A Wake-
619 Promoting Circadian Output Circuit in *Drosophila*. *Curr. Biol.* 28, 3098–3105.e3.

- 620 Li, M.-T., Cao, L.-H., Xiao, N., Tang, M., Deng, B., Yang, T., Yoshii, T., and Luo, D.-G.
621 (2018). Hub-organized parallel circuits of central circadian pacemaker neurons for visual
622 photoentrainment in *Drosophila*. *Nat. Commun.* *9*, 4247.
- 623 Li, Y., Guo, F., Shen, J., and Rosbash, M. (2014). PDF and cAMP enhance PER stability in
624 *Drosophila* clock neurons. *Proc. Natl. Acad. Sci. U. S. A.* *111*, E1284–E1290.
- 625 Lucas, R.J., Lall, G.S., Allen, A.E., and Brown, T.M. (2012). How rod, cone, and melanopsin
626 photoreceptors come together to enlighten the mammalian circadian clock. *Prog. Brain Res.*
627 *199*, 1–18.
- 628 Lucassen, E.A., van Diepen, H.C., Houben, T., Michel, S., Colwell, C.S., and Meijer, J.H.
629 (2012). Role of vasoactive intestinal peptide in seasonal encoding by the suprachiasmatic
630 nucleus clock. *Eur. J. Neurosci.* *35*, 1466–1474.
- 631 Mazzoni, E.O., Celik, A., Wernet, M.F., Vasiliauskas, D., Johnston, R.J., Cook, T.A.,
632 Pichaud, F., and Desplan, C. (2008). Iroquois complex genes induce co-expression of
633 rhodopsins in *Drosophila*. *PLoS Biol.* *6*, e97.
- 634 Menegazzi, P., Dalla Benetta, E., Beauchamp, M., Schlichting, M., Steffan-Dewenter, I., and
635 Helfrich-Förster, C. (2017). Adaptation of Circadian Neuronal Network to Photoperiod in
636 High-Latitude European *Drosophilids*. *Curr. Biol.* *27*, 833–839.
- 637 Meng, D., Li, H.-Q., Deisseroth, K., Leutgeb, S., and Spitzer, N.C. (2018). Neuronal activity
638 regulates neurotransmitter switching in the adult brain following light-induced stress. *Proc.*
639 *Natl. Acad. Sci. U. S. A.* *115*, 5064–5071.
- 640 Mertens, I., Vandingenen, A., Johnson, E.C., Shafer, O.T., Li, W., Trigg, J.S., De Loof, A.,
641 Schoofs, L., and Taghert, P.H. (2005). PDF receptor signaling in *Drosophila* contributes to
642 both circadian and geotactic behaviors. *Neuron* *48*, 213–219.
- 643 Muraro, N.I., and Ceriani, M.F. (2015). Acetylcholine from Visual Circuits Modulates the
644 Activity of Arousal Neurons in *Drosophila*. *J. Neurosci.* *35*, 16315–16327.
- 645 Port, F., and Bullock, S.L. (2016). Augmenting CRISPR applications in *Drosophila* with
646 tRNA-flanked sgRNAs. *Nat. Methods* *13*, 852–854.
- 647 Renn, S.C., Park, J.H., Rosbash, M., Hall, J.C., and Taghert, P.H. (1999). A pdf neuropeptide
648 gene mutation and ablation of PDF neurons each cause severe abnormalities of behavioral
649 circadian rhythms in *Drosophila*. *Cell* *99*, 791–802.
- 650 Rieger, D., Stanewsky, R., and Helfrich-Förster, C. (2003). Cryptochrome, compound eyes,
651 Hofbauer-Buchner eyelets, and ocelli play different roles in the entrainment and masking
652 pathway of the locomotor activity rhythm in the fruit fly *Drosophila melanogaster*. *J. Biol.*
653 *Rhythms* *18*, 377–391.
- 654 Rieger, D., Shafer, O.T., Tomioka, K., and Helfrich-Förster, C. (2006). Functional analysis of
655 circadian pacemaker neurons in *Drosophila melanogaster*. *J. Neurosci.* *26*, 2531–2543.
- 656 Rieger, D., Wülbeck, C., Rouyer, F., and Helfrich-Förster, C. (2009). *Period* Gene
657 Expression in Four Neurons Is Sufficient for Rhythmic Activity of *Drosophila melanogaster*
658 under Dim Light Conditions. *J. Biol. Rhythms* *24*, 271–282.

- 659 Rister, J., Desplan, C., and Vasiliasuskas, D. (2013). Establishing and maintaining gene
660 expression patterns: insights from sensory receptor patterning. *Development* 140, 493–503.
- 661 Schlichting, M., and Helfrich-Förster, C. (2015). Photic entrainment in *Drosophila* assessed
662 by locomotor activity recordings. *Methods Enzymol.* 552, 105–123.
- 663 Schlichting, M., Grebler, R., Peschel, N., Yoshii, T., and Helfrich-Förster, C. (2014).
664 Moonlight detection by *Drosophila*'s endogenous clock depends on multiple photopigments
665 in the compound eyes. *J. Biol. Rhythms* 29, 75–86.
- 666 Schlichting, M., Grebler, R., Menegazzi, P., and Helfrich-Förster, C. (2015). Twilight
667 dominates over moonlight in adjusting *Drosophila*'s activity pattern. *J. Biol. Rhythms* 30,
668 117–128.
- 669 Schlichting, M., Menegazzi, P., Lelito, K.R., Yao, Z., Buhl, E., Dalla Benetta, E., Bahle, A.,
670 Denike, J., Hodge, J.J., Helfrich-Förster, C., et al. (2016). A Neural Network Underlying
671 Circadian Entrainment and Photoperiodic Adjustment of Sleep and Activity in *Drosophila*. *J.*
672 *Neurosci.* 36, 9084–9096.
- 673 Schlichting, M., Menegazzi, P., Rosbash, M., and Helfrich-Förster, C. (2019). A distinct
674 visual pathway mediates high light intensity adaptation of the circadian clock in *Drosophila*.
675 *J. Neurosci.*
- 676 Schmid, B., Helfrich-Förster, C., and Yoshii, T. (2011). A new ImageJ plug-in “ActogramJ”
677 for chronobiological analyses. *J. Biol. Rhythms* 26, 464–467.
- 678 Schubert, F.K., Hagedorn, N., Yoshii, T., Helfrich-Förster, C., and Rieger, D. (2018).
679 Neuroanatomical details of the lateral neurons of *Drosophila melanogaster* support their
680 functional role in the circadian system. *J. Comp. Neurol.* 526, 1209–1231.
- 681 Shafer, O.T., and Taghert, P.H. (2009). RNA-interference knockdown of *Drosophila* pigment
682 dispersing factor in neuronal subsets: the anatomical basis of a neuropeptide's circadian
683 functions. *PLoS One* 4, e8298.
- 684 Shang, Y., Griffith, L.C., and Rosbash, M. (2008). Light-arousal and circadian
685 photoreception circuits intersect at the large PDF cells of the *Drosophila* brain. *Proc. Natl.*
686 *Acad. Sci. U. S. A.* 105, 19587–19594.
- 687 Sprecher, S.G., and Desplan, C. (2008). Switch of rhodopsin expression in terminally
688 differentiated *Drosophila* sensory neurons. *Nature* 454, 533–537.
- 689 Stanewsky, R., Kaneko, M., Emery, P., Beretta, B., Wager-Smith, K., Kay, S.A., Rosbash,
690 M., and Hall, J.C. (1998). The *cryb* mutation identifies cryptochrome as a circadian
691 photoreceptor in *Drosophila*. *Cell* 95, 681–692.
- 692 Stoleru, D., Peng, Y., Agosto, J., and Rosbash, M. (2004). Coupled oscillators control
693 morning and evening locomotor behaviour of *Drosophila*. *Nature* 431, 862–868.
- 694 Tahayato, A., Sonnevile, R., Pichaud, F., Wernet, M.F., Papatsenko, D., Beaufils, P., Cook,
695 T., and Desplan, C. (2003). Otd/Crx, a Dual Regulator for the Specification of Ommatidia
696 Subtypes in the *Drosophila* Retina. *Dev. Cell* 5, 391–402.

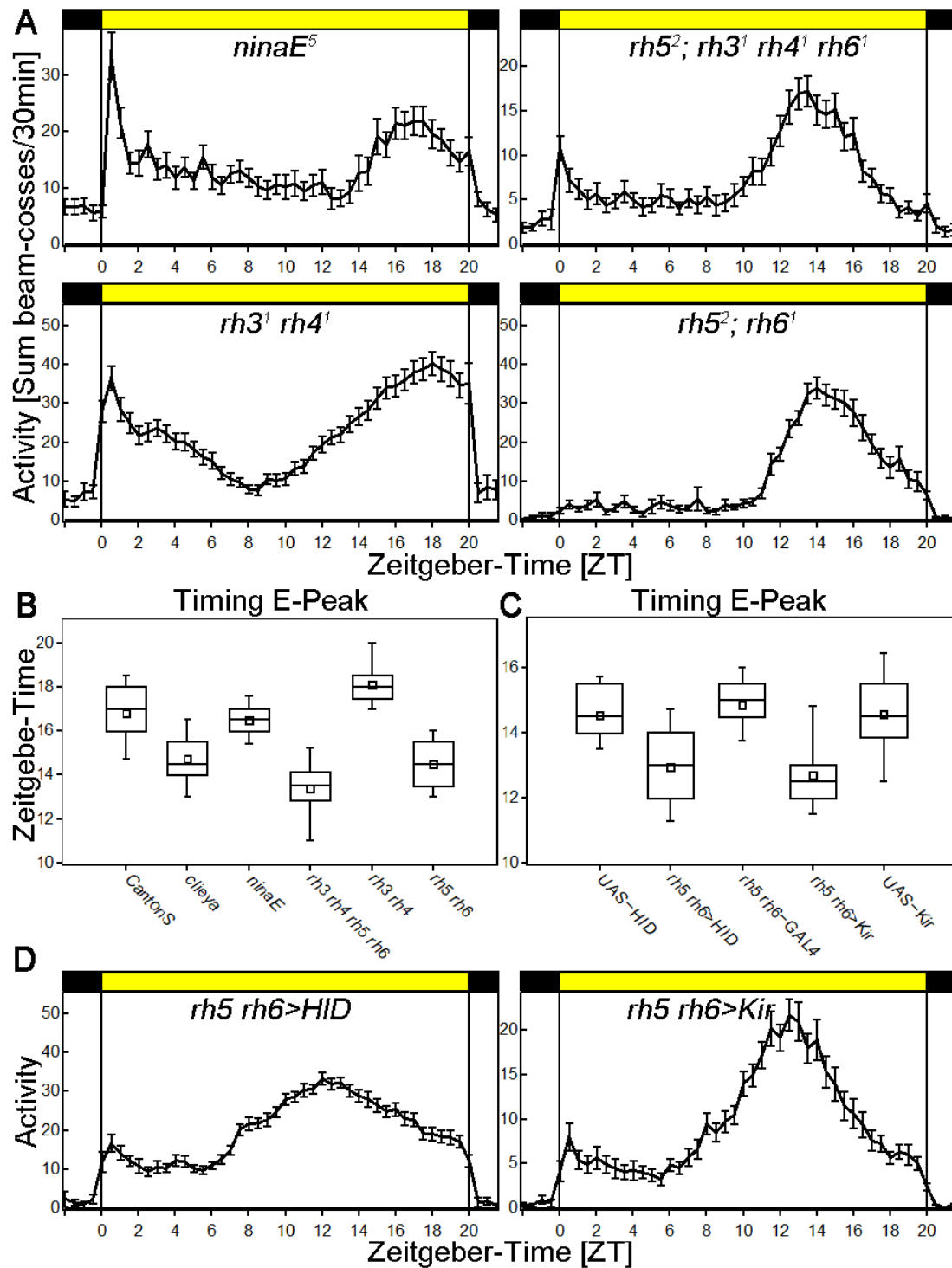
- 697 Vasiliauskas, D., Mazzoni, E.O., Sprecher, S.G., Brodetskiy, K., Johnston, R.J., Jr, Lidder, P.,
698 Vogt, N., Celik, A., and Desplan, C. (2011). Feedback from rhodopsin controls rhodopsin
699 exclusion in *Drosophila* photoreceptors. *Nature* 479, 108–112.
- 700 Wernet, M.F., Mazzoni, E.O., Çelik, A., Duncan, D.M., Duncan, I., and Desplan, C. (2006).
701 Stochastic spineless expression creates the retinal mosaic for colour vision. *Nature* 440, 174–
702 180.
- 703 Yamaguchi, S., Wolf, R., Desplan, C., and Heisenberg, M. (2008). Motion vision is
704 independent of color in *Drosophila*. *Proc. Natl. Acad. Sci. U. S. A.* 105, 4910–4915.
- 705 Yoshii, T., Wülbeck, C., Sehadova, H., Veleri, S., Bichler, D., Stanewsky, R., and Helfrich-
706 Förster, C. (2009). The neuropeptide pigment-dispersing factor adjusts period and phase of
707 *Drosophila*'s clock. *J. Neurosci.* 29, 2597–2610.
- 708 Yoshii, T., Hermann-Luibl, C., and Helfrich-Förster, C. (2016). Circadian light-input
709 pathways in *Drosophila*. *Commun. Integr. Biol.* 9, e1102805.
- 710

711 **Figure 1**



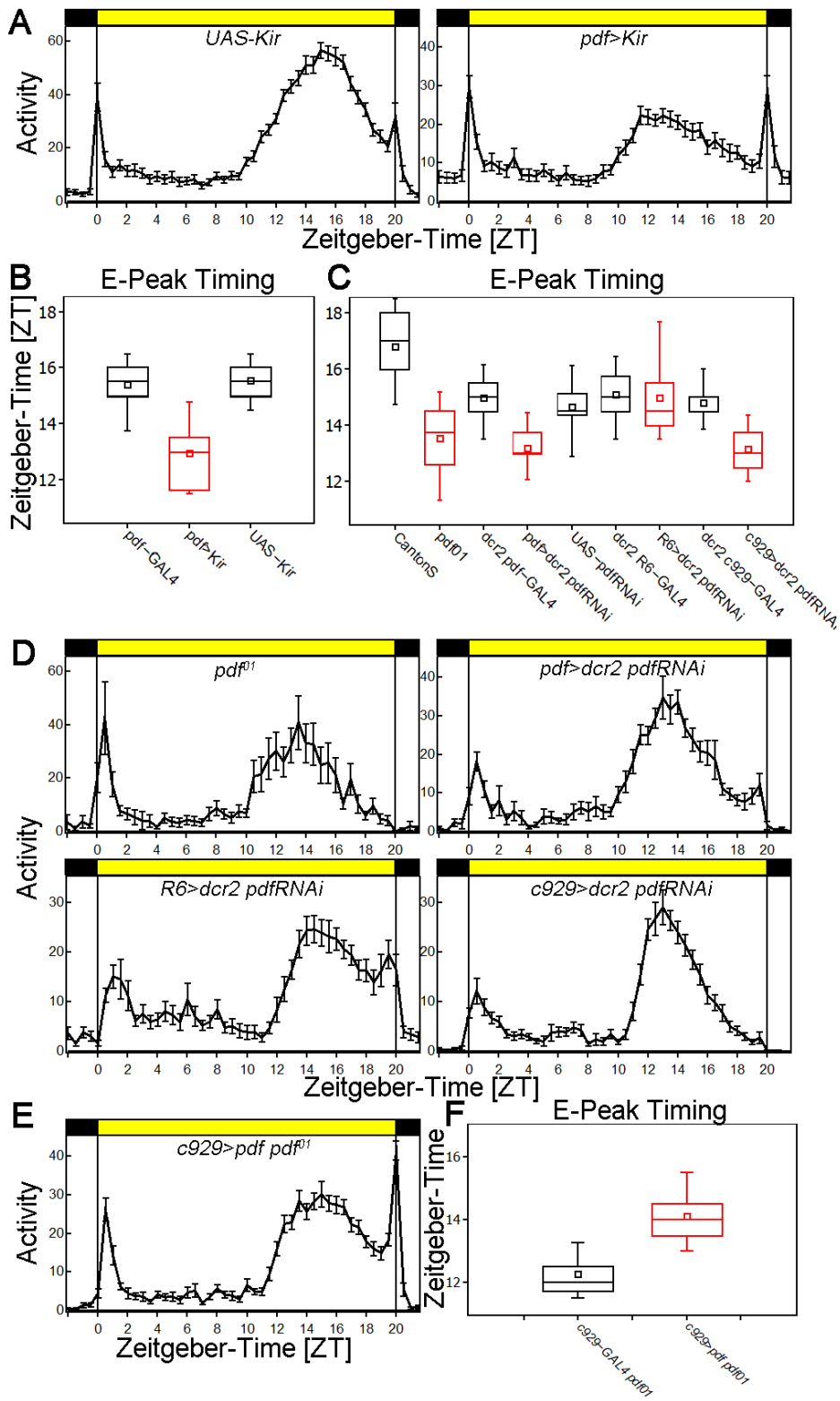
712

713 **Figure 2**



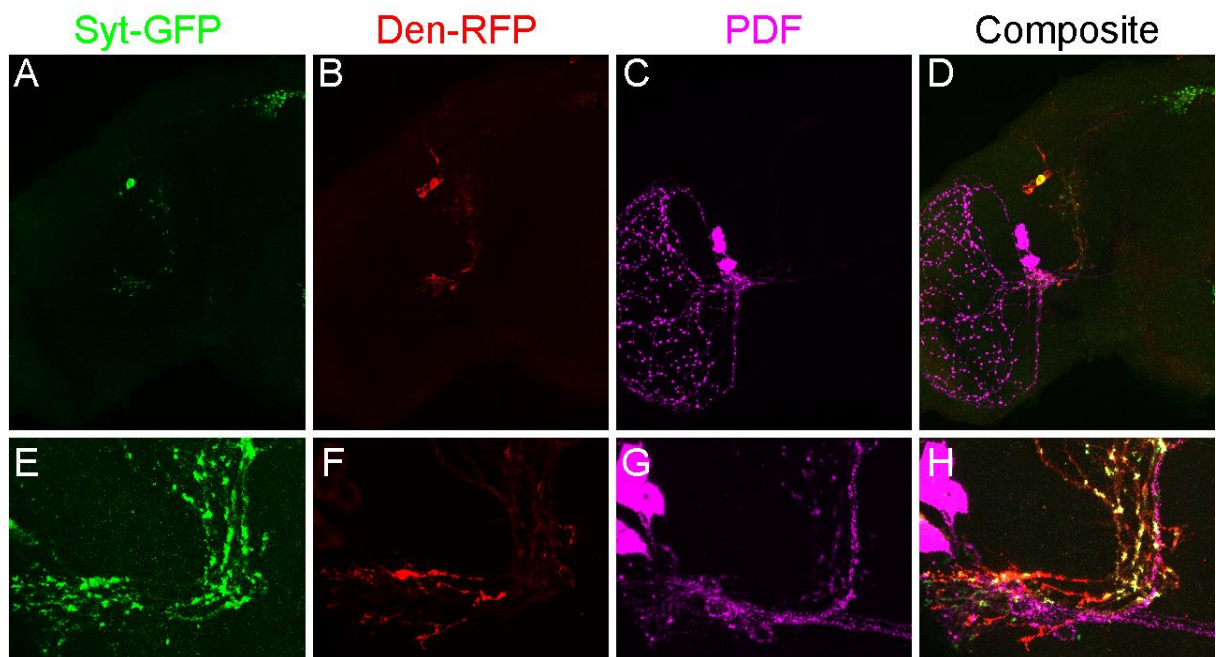
714

715 **Figure 3**



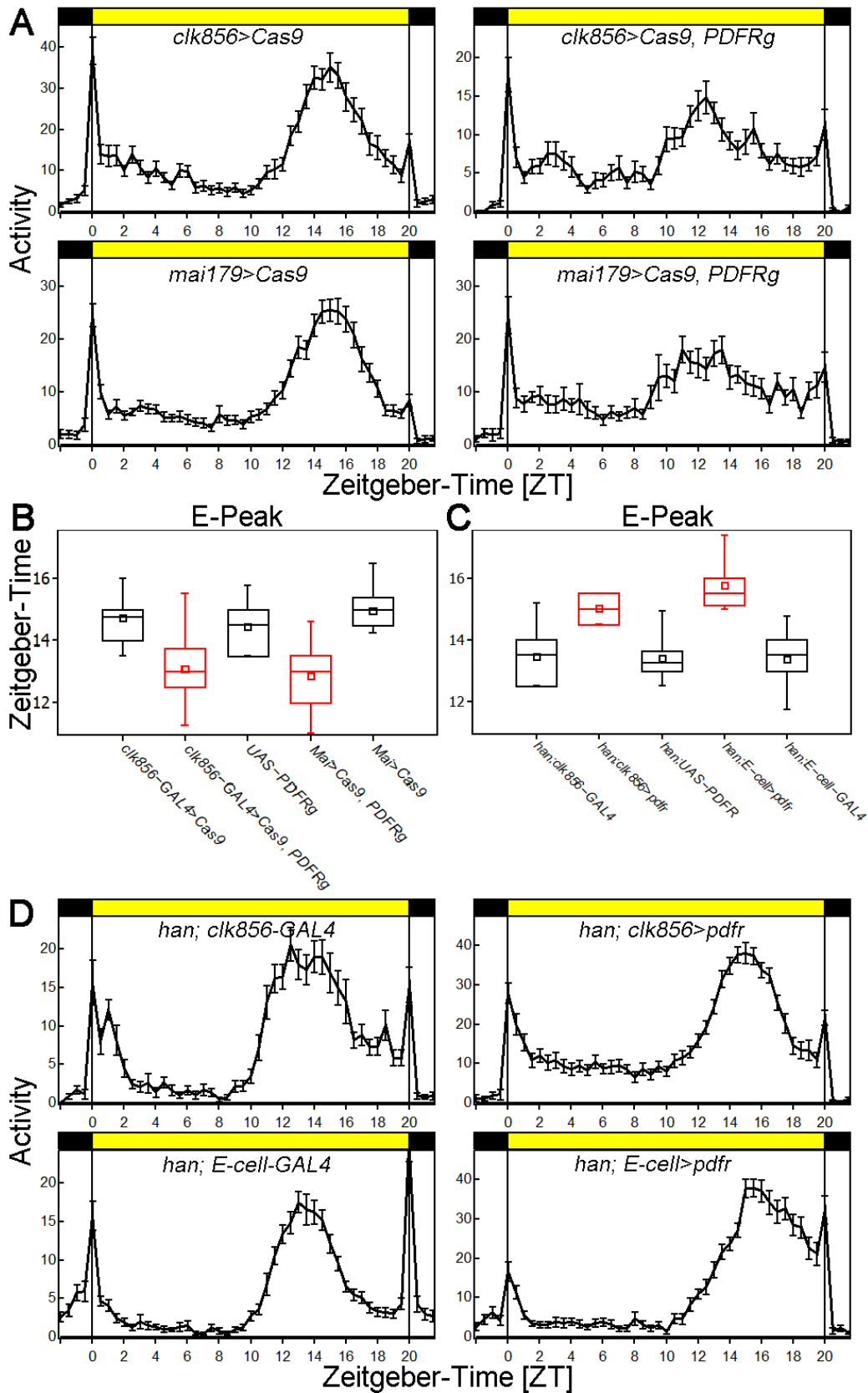
716

717 **Figure 4**



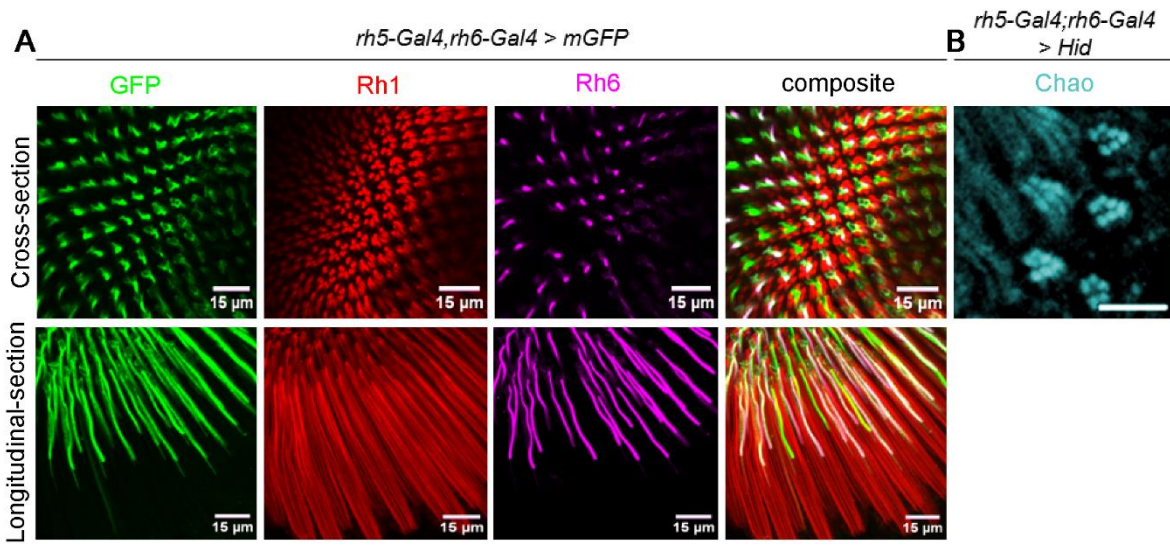
718

719 **Figure 5**



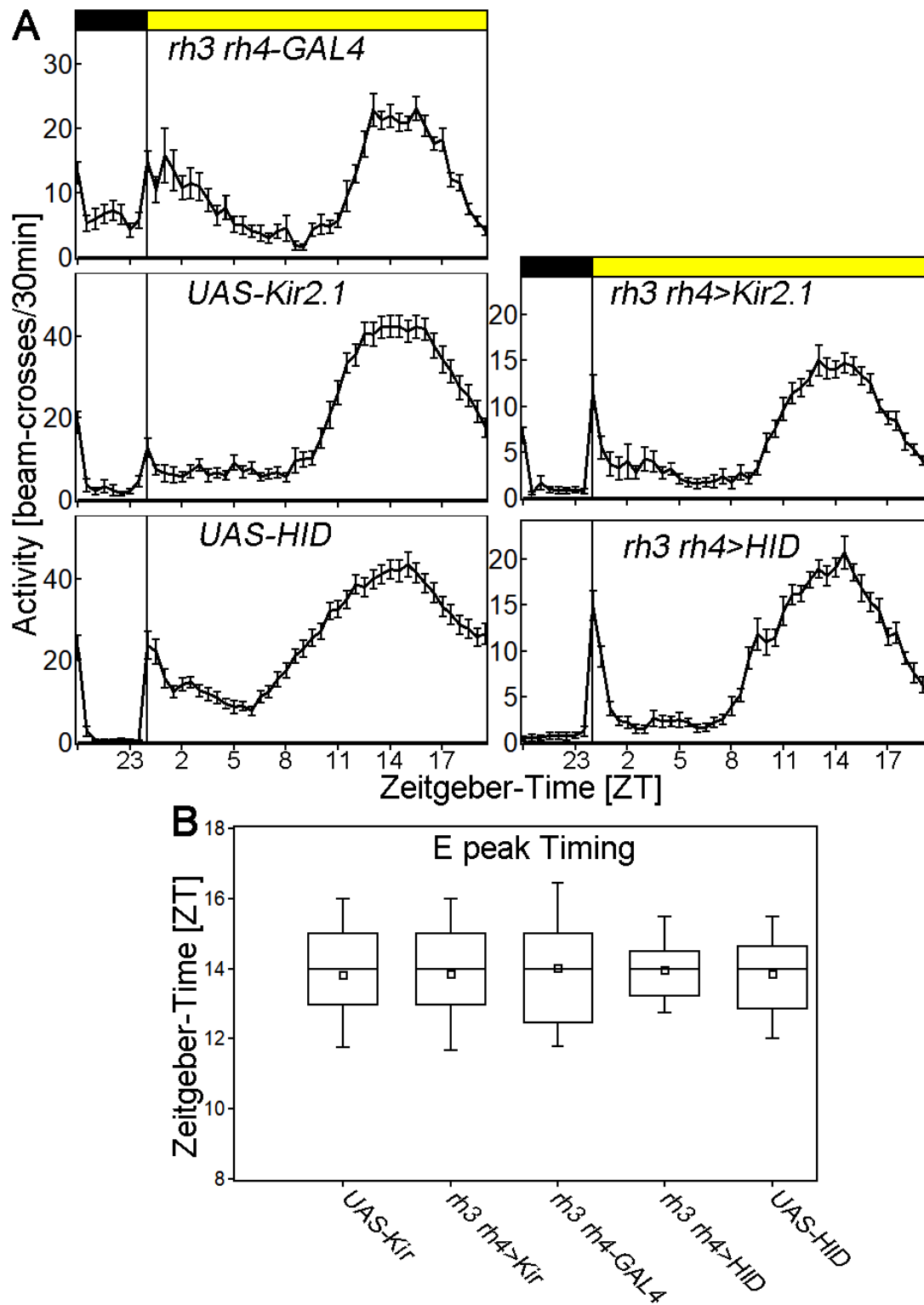
720

721 **Suppl Figure 1**



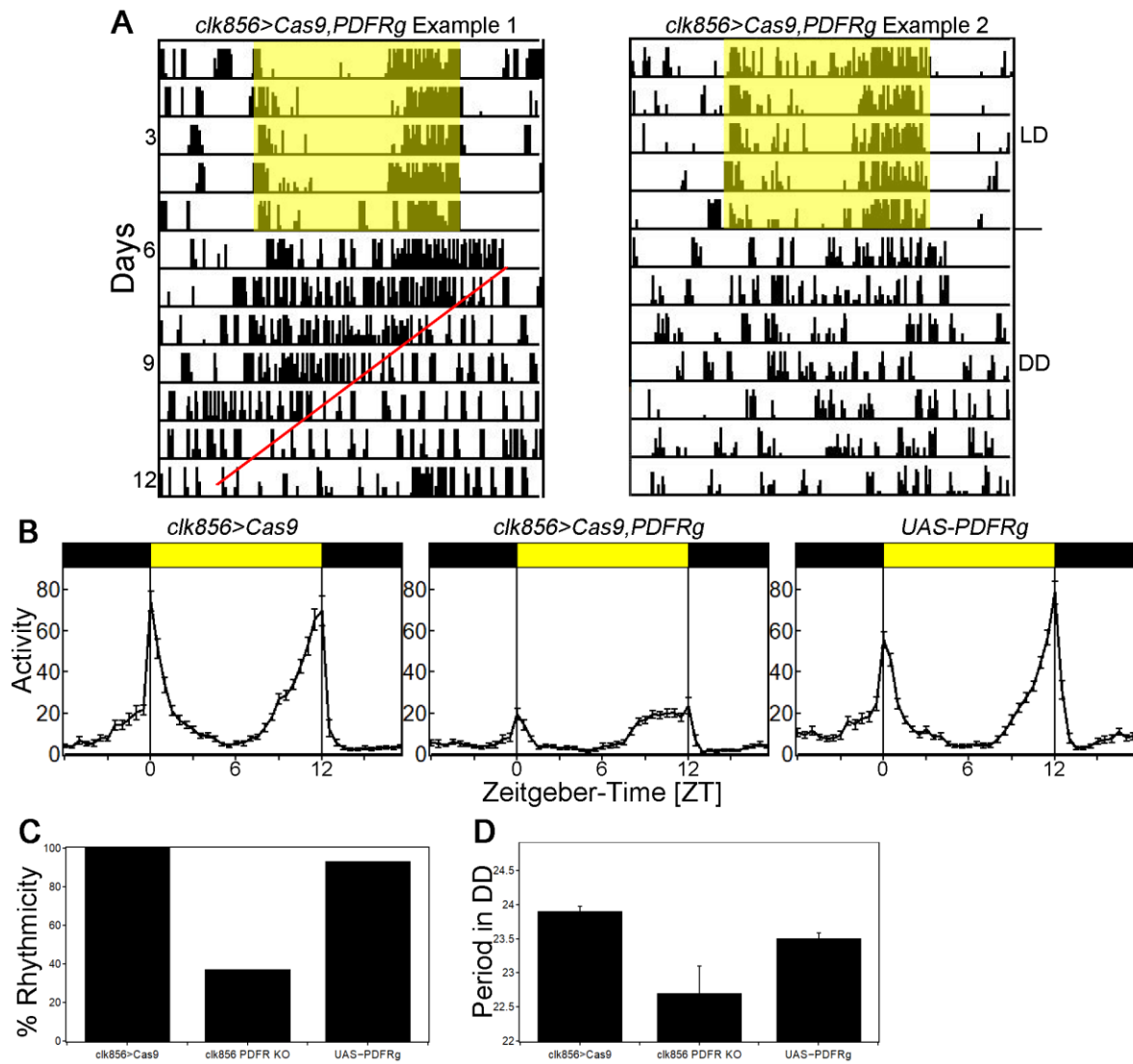
722

723 Suppl Figure 2



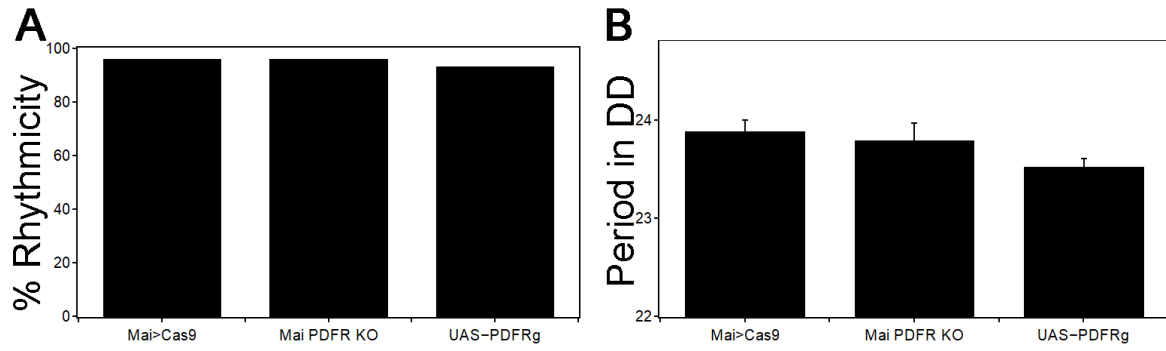
724

725 **Suppl. Figure 3**



726

727 **Suppl. Figure 4**



728